A Dynamical Linkage Between Western North Pacific Tropical Cyclones and Indian Monsoon Low-Pressure Systems

K. S. S. Sai Srujan[1], Sukumaran Sandeep[1], Ettammal suhas[2], and Hariprasad Kodamana[1]

[1]Indian Institute of Technology Delhi
[2]Indian Institute of Science Education and Research Pune

November 26, 2022

Abstract

The relatively weak tropical storms, known as low-pressure systems (LPSs), contribute as much as 60% of the seasonal precipitation over the hugely populated central India. More than a third of LPS are formed by the downstream amplification of the westward propagating disturbances from the Pacific. Here, we show that the downstream LPS genesis are associated with the tropical cyclones (TCs) in the Western North Pacific (WNP). Four major clusters of landfalling TCs that have a relatively lesser degree of recurvature account for about 83% of the downstream LPS genesis. Causality in the fluctuations of the sea level pressure over the Bay of Bengal (BoB) prior to the initiation of LPS is attributed to the Rossby wave activity over WNP through transfer entropy analysis. Our results suggest a potential for the prediction of the downstream synoptic activity over the BoB at least seven days ahead.

A Dynamical Linkage Between Western North Pacific Tropical Cyclones and Indian Monsoon Low-Pressure Systems

K. S. S. Sai Srujan[1], S. Sandeep[1], E. Suhas[2], and Hariprasad Kodamana[3,4]

[1]Centre for Atmospheric Sciences, Indian Institute of Technology Delhi, New Delhi 110016, India
[2]Earth and Climate Science, Indian Institute of Science Education and Research Pune, Pune 411 008, India
[3]Department of Chemical Engineering, Indian Institute of Technology Delhi, New Delhi 110016, India
[4]School of Artificial Intelligence, Indian Institute of Technology Delhi, New Delhi 110016, India

Key Points:

- A causal relationship is found between atmospheric Rossby wave activity over Pacific and sea-level pressure variation over the Bay of Bengal
- Landfalling tropical cyclones over the South China Sea are associated with low-pressure systems' genesis over the Bay of Bengal
- 83% of downstream low-pressure systems over the Bay of Bengal are linked to four tropical cyclone clusters over Western North Pacific

Corresponding author: S. Sandeep, `sandeep.sukumaran@cas.iitd.ac.in`

Abstract

The relatively weak tropical storms, known as low-pressure systems (LPSs), contribute as much as 60% of the seasonal precipitation over the hugely populated central India. More than a third of LPS are formed by the downstream amplification of the westward propagating disturbances from the Pacific. Here, we show that the downstream LPS genesis are associated with the tropical cyclones (TCs) in the Western North Pacific (WNP). Four major clusters of landfalling TCs that have a relatively lesser degree of recurvature account for about 83% of the downstream LPS genesis. Causality in the fluctuations of the sea level pressure over the Bay of Bengal (BoB) prior to the initiation of LPS is attributed to the Rossby wave activity over WNP through transfer entropy analysis. Our results suggest a potential for the prediction of the downstream synoptic activity over the BoB at least seven days ahead.

Plain Language Summary

The monsoon low-pressure systems (LPSs) are cyclonic vortices of diameter 1000–2000 km that are predominantly present over the Bay of Bengal (BoB) during the summer monsoon. These systems are responsible for more than half of the summer monsoon rainfall over the highly populated central India and Gangetic plains. The genesis mechanisms of monsoon LPS are not fully understood, but can be broadly classified into two types - local processes (in situ) and remote forcing by the westward propagating atmospheric disturbances from the Pacific (downstream amplification). In this study, we show that the Rossby waves from four clusters of Western North Pacific (WNP) tropical cyclones (TCs) might be responsible for the triggering of most of the downstream genesis of the synoptic-scale storms over the BoB during the summer monsoon season. Our results suggest that the downstream storm development over the BoB can be reliably predicted, possibly using deep learning models, by considering predictors from WNP.

1 Introduction

The monsoon low-pressure systems (LPSs) are synoptic-scale vortices embedded in the large-scale South Asian summer monsoon circulation. These precipitating vortices produce more than half of the summer monsoon rainfall over Central India (Praveen et al., 2015; Krishnamurthy & Ajayamohan, 2010; Hunt & Fletcher, 2019; Thomas et al., 2021; Deoras et al., 2021). The weak cyclonic vortices that form over the Bay of Bengal (BoB) during summer monsoon season(June to September) has been reported more than a century ago (e.g., Eliot (1884), Blanford, (1890)). The trajectories of LPS have been archived since the late 19$^{\text{th}}$ century using the surface pressure charts by India Meteorological Department (IMD) [e.g., Mooley and Shukla, 1986; Sikka, 2006]. However, there is no clear understanding of the genesis mechanisms of LPS (Boos et al., 2015; Cohen & Boos, 2016). Previous attempts to study LPS genesis have examined the roles of baroclinic, barotropic, and combined barotropic-baroclinic instabilities (Shukla, 1977, 1978; Mishra & Salvekar, 1980; Lindzen et al., 1983). None of those studies were able to explain the observed genesis and growth of LPS adequately (Cohen & Boos, 2016). It is also noted that these studies did not distinguish mechanisms of downstream and in-situ formation of LPS. Although dynamic and thermodynamic structures of in-situ and downstream LPS are found to be similar, processes leading to their genesis are different . Hence the formation mechanisms of the two types of LPS should be addressed separately (Meera et al., 2019). The lack of distinction between downstream and in situ genesis might be one of the reasons for the inadequate understanding of the LPS genesis.

In the in-situ LPS genesis events, the local dynamics and thermodynamics controls the formation of the vortex, whereas in the downstream case, westward propagating atmospheric disturbances from the western north Pacific (WNP) can trigger a downstream amplification over the BoB (Krishnamurti et al., 1977). Most of the earlier studies in the pre-satellite era assumed in-situ formation of LPS over the BoB, except for a few studies which reported the classification of genesis mechanisms (Krishnamurti et al., 1977; K. Saha et al., 1981; Chen & Weng, 1999). However, the studies that classified LPS on the basis of genesis mechanisms attributed more than 80% of the genesis to downstream amplification (Krishnamurti et al., 1977; K. Saha et al., 1981; Chen & Weng, 1999). Recently Meera et al. (2019), with the help of a long-term data analysis, have shown that only 32% of the LPS forms through downstream amplification and the remaining are in-situ genesis. The relatively shorter period of analysis in the earlier studies might be the reason for the differences in the ratio of in situ to downstream LPS genesis between earlier and recent studies. Irrespective of the ratio of the in-situ to downstream LPS, the two types of systems should be treated separately to have a clear understanding of the genesis.

The relationship between WNP TC activity and the Indian summer monsoon has been investigated in the past. However, the results were contradictory, with some suggesting a weakening of monsoon circulation and precipitation in response to excessive TC activity while others argued that WNP TCs are favorable for downstream LPS genesis that in turn can strengthen the monsoon precipitation (Krishnamurti et al., 1977; Kanamitsu & Krishnamurti, 1978; Chen & Weng, 1999). Krishnamurti et al. (1977) suggested that the westward propagating shortwaves associated with WNP TCs might be responsible for the downstream amplification of LPS over the BoB. Further, their analysis suggested that TCs making landfall over the east China coast trigger westward propagating waves. However, the nature of TCs responsible for the triggering of downstream amplification is not fully investigated. Further, K. Saha et al. (1981) considered only July and August for their analysis, while a large number of LPS forms in June and September as well (Meera et al., 2019). An analysis covering the entire summer monsoon season (June – September) is necessary to fully understand the downstream amplification of LPS. Here, following Camargo et al. (2007), we identify TC clusters in order to better understand the nature of link between WNP TC and Indian monsoon LPS activity. Similar analysis robustly established the relationship between TC clusters and Madden–Julian Oscillation and El Niño Southern Oscillation (Camargo et al., 2007, 2008). The link between WNP TC clusters and downstream amplification might lead to a better predictability of LPS genesis over the BoB. The main objective of the present study is to establish a cause-effect relationship (and thereby the existence of predictability) between WNP TCs activity and downstream genesis of LPS over the BoB.

2 Data and Methodology

The best track dataset provided by the Joint Typhoon Warning Center (JTWC) from 1979–2017 at a six hour interval over WNP basin are considered for the analysis. Only those systems that are categorised as a tropical storm or higher category during June-September are considered for the analysis. The daily mean sea-level pressure (MSLP) of European Centre for Medium-Range Weather Forecasts fifth generation (ERA5) reanalysis dataset (Hersbach et al., 2020) at a spatial resolution of 0.25°x0.25° from 1979–2017 is used in this study. The LPS are tracked using the algorithm developed by Praveen et al. (2015) from ERA5 which include all categories of LPS over BoB. The identified LPS are broadly classified into in-situ and downstream using the algorithm proposed by Srujan et al. (2021) which is an automation of the classification technique used by Meera et al. (2019).

Convectively coupled equatorial waves are identified by performing wave number-frequency power spectral analysis on National Oceanographic and Atmospheric Administration interpolated daily outgoing longwave radiation (OLR) data (Liebmann & Smith, 1996) and fitting the theoretical dispersion relationship for each wave mode by adjusting the equivalent depth (Murakami, 1980; Wheeler & Kiladis, 1999). Significant $n = 1$ Rossby wave amplitude was observed between equivalent depth 10 m and 100 m for wave number -10 and -2 and period 8 and 90 days (Fig. S1) and hence, Rossby waves in OLR are isolated by applying wave number-frequency filtering in these region. An Emperical Orthogonal Function (EOF) analysis is performed on the Rossby wave filtered daily OLR anomalies over the domain 100°E–180°E, 0°–20°N. The leading principal component (PC1) explains the Rossby wave activity over this region. The transfer entropy (TE), which is a measure to quantify the information transferred from one variable to another variable, is calculated between the PC1 and the MSLP over the domain 90°E – 120°E, 15°N25°N (Schreiber, 2000; Kaiser & Schreiber, 2002; Lizier et al., 2008). To examine the existence of any predictive relationship between PC1 and MSLP, the TE is calculated for time lags ranging from zero to seven days by sliding the PC1 time series. The TE computations are repeated three times for each lag by increasing the length of the time series by one day for each calculation. For instance, at lag-0, the TE is computed initially by taking PC1 and MSLP time series from t-4 to t+2 days, where t-0 is the date of initiation of a downstream LPS. This calculation is then repeated two more time by changing the start date to t-5 and t-6, respectively. This is done to examine the sensitivity of TE calculations to the length of the time series. For lags 1 to 7, the length of the data for TE calculation is increased by adding the lag.

The WNP TCs are divided into six clusters using the mixture polynomial regression model to fit the trajectories of TCs (Gaffney, 2004; Camargo et al., 2007, 2008). The log-likelihood is the measure of goodness-of-fit for the probabilistic mixture models; therefore the log-likelihood values verses the number of clusters curve is shown (Fig. S2) . The number of clusters are selected on the basis of a threshold log-likelihood (Δl) value 0.05. The termination of clusters happens when Δl value falls below the threshold value for two consecutive times. The Δl values between clusters 6,7 and clusters 7,8 are less than 0.05, and therefore a total of six clusters are considered (Fig. S2).

3 Results and discussion

The total monthly occurrences of WNP TCs and the two categories of LPS over the Indian monsoon region from 1979 to 2017 are shown in Fig. 1. The TC occurrences are minimum in June followed by a doubling in July. The maximum TC genesis is found in August followed by September. The distribution of number of monthly downstream LPS follows the similar pattern as WNP TC distribution, except for closer genesis numbers between June and July, indicating a link between them. It is clear from Fig. 1 that downstream LPS cases are more prominent in the months of August and September, similar to the distribution of TC frequency. The earlier analysis on this topic was confined to July and August (K. Saha et al., 1981). The distribution of in-situ LPS genesis numbers is different from those of downstream LPS and TCs. Many previous studies considered topical cyclones as an important source of synoptic scale wave activity over WNP region (Krishnamurti et al., 1977; Sobel & Bretherton, 1999; Tam & Li, 2006). It is hypothesized that Rossby wave energy dispersion from a preexisting cyclone could trigger synoptic scale disturbances. Confluent background flow over the west Pacific also acts as a conductive environment for the genesis of synoptic scale wave disturbances through wave energy accumulation (Webster & Chang, 1988). A strong Rossby wave activity can be seen in the WNP during June - September season (Fig. S3). A clear westward propagation of the relative vorticity (ζ) anomaly and low-level winds can also be seen around 120°E towards the BoB (Fig. S4). A regression of PC1 of Rossby filtered OLR on 850 hPa wind vectors at different lags shows a westward propagation of disturbance from WNP and an intensification of the cyclonic circulation over the BoB (Fig. S5).

The earlier studies did not establish a causality of downstream LPS to signals propagating from the WNP (Krishnamurti et al., 1977; K. Saha et al., 1981; Chen & Weng, 1999; Meera et al., 2019). We establish the causal relationship between the Rossby variance over the West Pacific and downstream LPS over the BoB using TE. The TE shows flow of information from the memory of one variable to the other variable (Gupta et al., 2020). The TE captures both the memory as well as direction of information compared to mutual information. Recently, Gupta et al. (2020) applied TE to check the information transferred between pollutants and meteorological variables. They have found a TE value of about 25 for a strong link between two parameters and that of 0.01 for a weak link. The high value of TE indicates the strength of information transfer. The TE is calculated considering MSLP over box-1 and PC1 of Rossby-filtered OLR anomaly over box-2 (Fig. S3). The TE from PC1 to MSLP is of the order of 10^9 in case of downstream LPS (Fig. 2a) while that of in situ LPS is much smaller (Fig. 2b), reinforcing the argument that in situ genesis is due to the local dynamics and thermodynamics. In the case of downstream LPS, although the TE magnitude fluctuates slightly for each lag, its order remains the same (Fig.2a). To examine the possibility of propagation of the signal in the opposite direction, viz, from the BoB to WNP, we computed TE from MSLP to PC1 which is found to be low. This suggests that the propagation of signal is only in the westward direction from WNP. Also, TE values are consistent when the calculation is repeated by varying the length of time series from 7 to 9 days which indicates the robustness of the result.

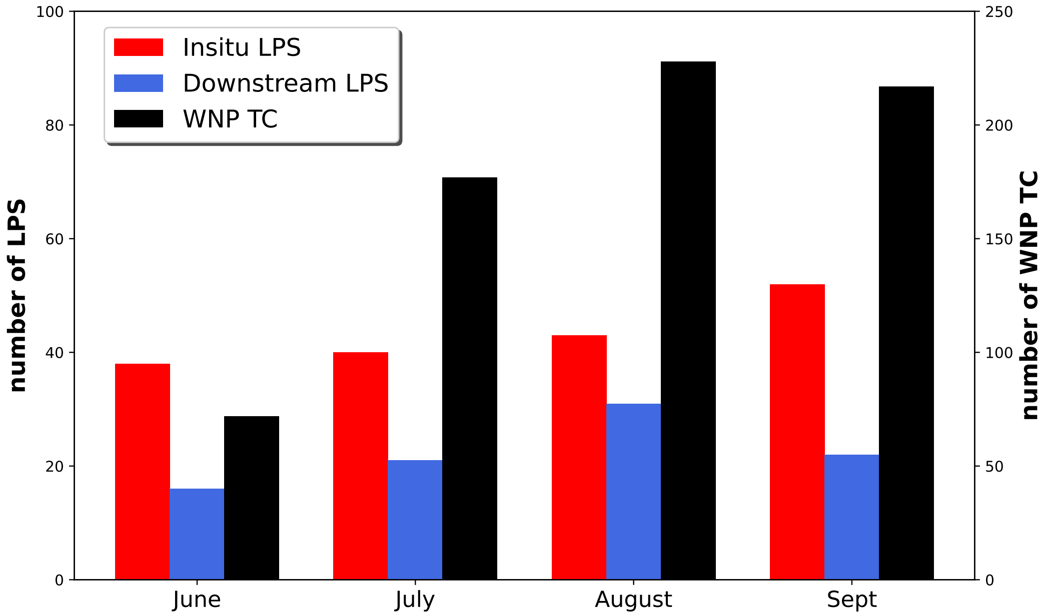

Figure 1. The total monthly distribution of Western North Pacific tropical cyclones, downstream, and in-situ low-pressure systems for the months of June, July, August, and September. The calculations are based on the data during 1979-2017 period. A Kolmogorov−Smirnov test rejected the null hypothesis that in-situ LPS and TCs have the same distribution ($p<0.05$) while the null hypothesis could not be rejected in the case of downstream LPS and TCs.

A clustering analysis of WNP TCs was carried out as suggested by Camargo et al. (2007), using a polynomial mixture model that fits geographical tracks. The polynomial mixture model is a probabilistic model which does soft clustering by assigning probabilities to each data point to which cluster it belongs. The Expectation-Maximization is used to optimize the model. The clustering analysis reveals six major TC clusters over the WNP (Fig. 3). As our focus is on monsoon LPS, we consider the summer monsoon season (June – September) for the TC clustering analysis. The mean track curve of all TC tracks in each cluster is shown. The clusters are labeled from A-F in which the cluster A contains the most number of TCs and cluster F the lowest. Most TCs in cluster A form west of 140°E and the mean track computed by interpolating all TCs in the cluster to 5 days suggests that they propagate in the northward direction in general with an angle of recurvature of 63.1°. The TC tracks in clusters B and D undergo minimal re-curvature. The angle of recurvature for the mean track of these two clusters is zero (Table S1). The TCs in cluster

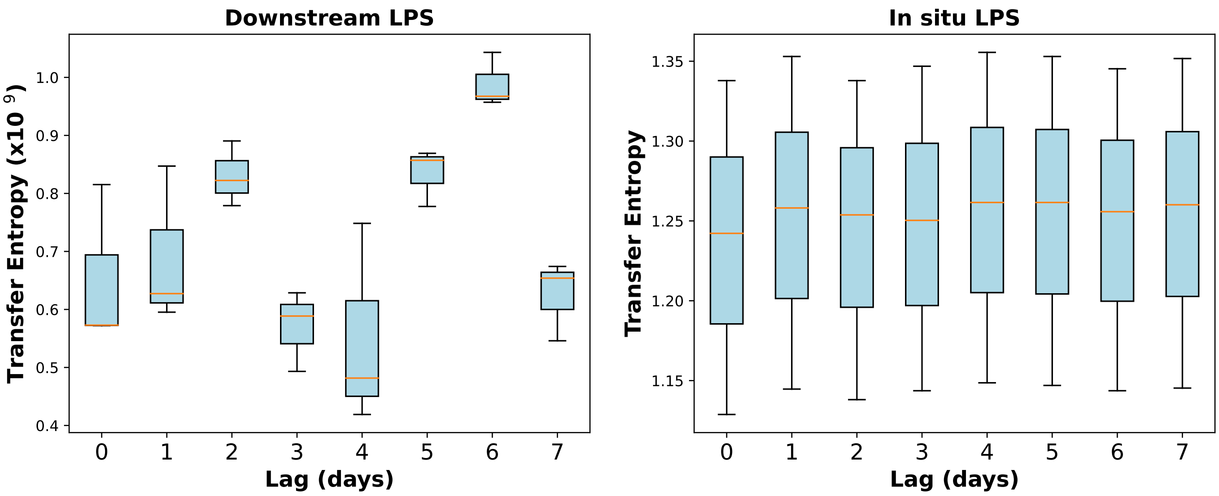

Figure 2. Transfer entropy between PC1 of Rossby filtered OLR over the WNP and MSLP over the BoB computed for (a) downstream and (b) in situ LPS at different lags. Lag-0 indicates that both the time series have the same start and end dates and with increasing lags, the PC1 time series is shifted ahead of a fixed MSLP time series. At each lag, the TE is computed three times by varying the length of the time series.

C are recurving in nature, with their genesis west of 140°E like that of TCs cluster A. The TCs in cluster C has a long westward moving trajectory before recurving at an angle of 87.5°. The TC tracks in clusters E and F are initiated in the tropical central Pacific and often the lifecycle of TCs in these clusters are longer compared to other clusters. The angle of recuravture of clusters E and F are 81.1° and 101.4°, respectively, with cluster F having a large angle of recurvature among all clusters. The landfall locations of cluster B and D TCs are somewhat similar though their origins are different, with cluster B TCs forming mostly west of 140°E and the latter east of 150°E. It is evident from the mean TC track in Fig. 3 that most of the TCs in clusters A, B, C, and D have large westward propagating component close to South China Sea.

The normalized monthly distributions of TCs in all six clusters for the JJAS season are shown in Fig. S6. The normalised monthly distribution of TC frequency in cluster A is identical with the total monthly distributions of WNP TCs and the downstream LPS as shown in Fig. 1. The relative TC genesis frequency is weak in June in all clusters except cluster D. The downstream LPS genesis is also least in the month of June. Although the distribution of total TCs are similar to that in Camargo et al. (2007), the distribution within the clusters are different which may be due to the difference in the season and number of clusters considered. The TCs in each cluster which trigger a downstream LPS have either large westward moving component or landfall close to South China sea and adjacent land area(Fig. S7). 83% of the downstream LPS genesis is associated with the TCs in clusters A, B, C, and D (Fig. S8). Further, the sum of monthly distributions of TCs in clusters A, B, C, and D show a pattern similar to the monthly distributions of downstream LPS. The detailed statistics of cluster-wise TCs are shown in Table S2. The percentage of TC landfall is very high in the cluster D (96%) followed by the cluster B (88%) and the least number of landfall occurs in the cluster E (3.75%) which is consistent with the trajectories in Fig. 3. The overall percentage of landfall is 43.6% which is in line with the estimates of Camargo et al. (2007) though analysis periods are different.

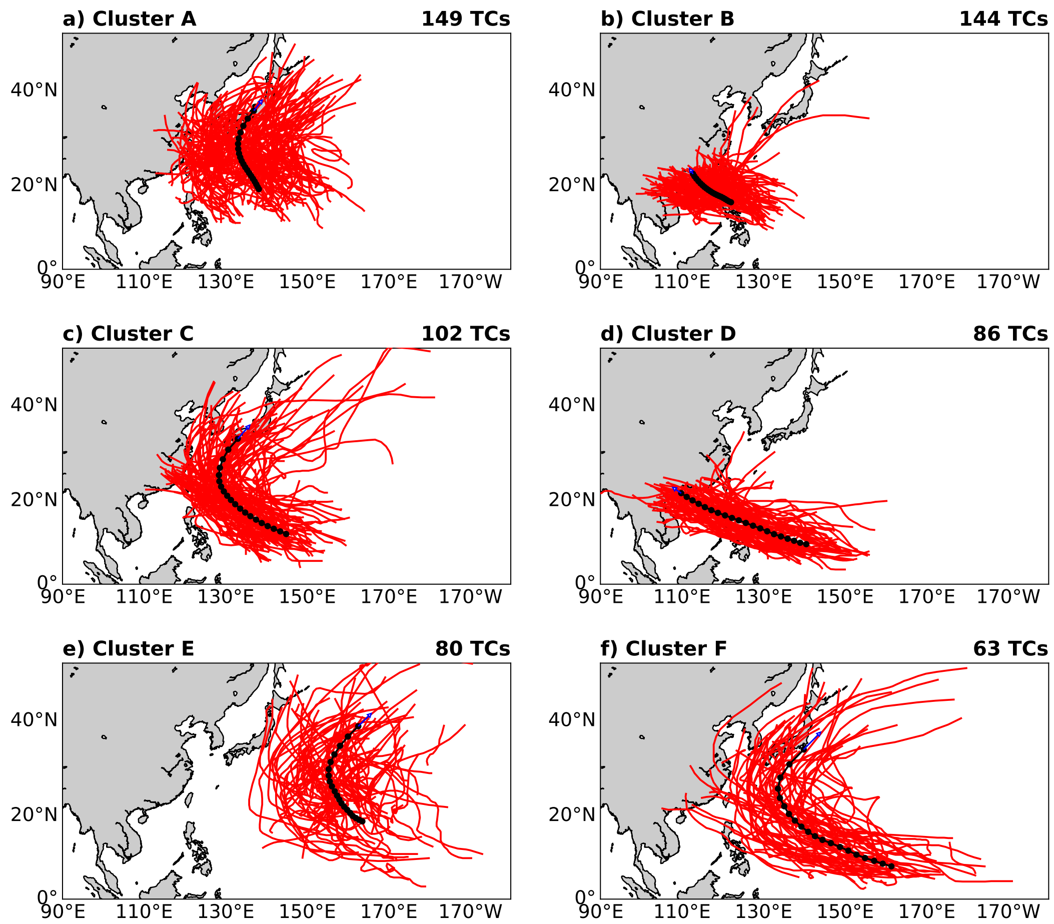

Figure 3. The total tracks of TCs over WNP from 1979-2017 in each cluster from A-F with the mean track(Black line) of TCs interpolated to a length of 5 days. The number of TC tracks in each cluster is indicated on top right side of the panels.

In order to understand the association between the downstream LPS genesis and the TCs in each cluster, we estimate the monthly number of LPS genesis within one to ten days of a TC genesis in each cluster (Fig. 4). The reason for choosing a 10-day window is because earlier studies suggested an average of 12 systems forming per June - September season that translates into one storm genesis in 10 days (Hurley & Boos, 2015). The total number of LPS genesis associated with each TC cluster is shown in Fig. 4a. TCs in clusters A to D account for 83% of the downstream LPS genesis. From Fig. 3, it is clear that TC genesis in clusters E and F happens closer to the dateline than that in other clusters. The monthly distribution of cluster-wise downstream LPS genesis frequency explains the monthly genesis of downstream LPS shown in Fig. 1. Most of the clusters show a weak or zero genesis of downstream LPS in the month of June. The most favorable months for downstream LPS genesis that is linked to a TC cluster are August and September, in line with the analysis shown in Fig. 1.

The degree of recurvature of TCs in clusters A, B, C, and D is less compared to that of E and F. Further, the frequency of TC landfall is more in the first four clusters. Krishnamurthi et al. (1977) have also suggested that the landfalling TCs over the eastern China coast trigger westward propagating atmospheric disturbances.

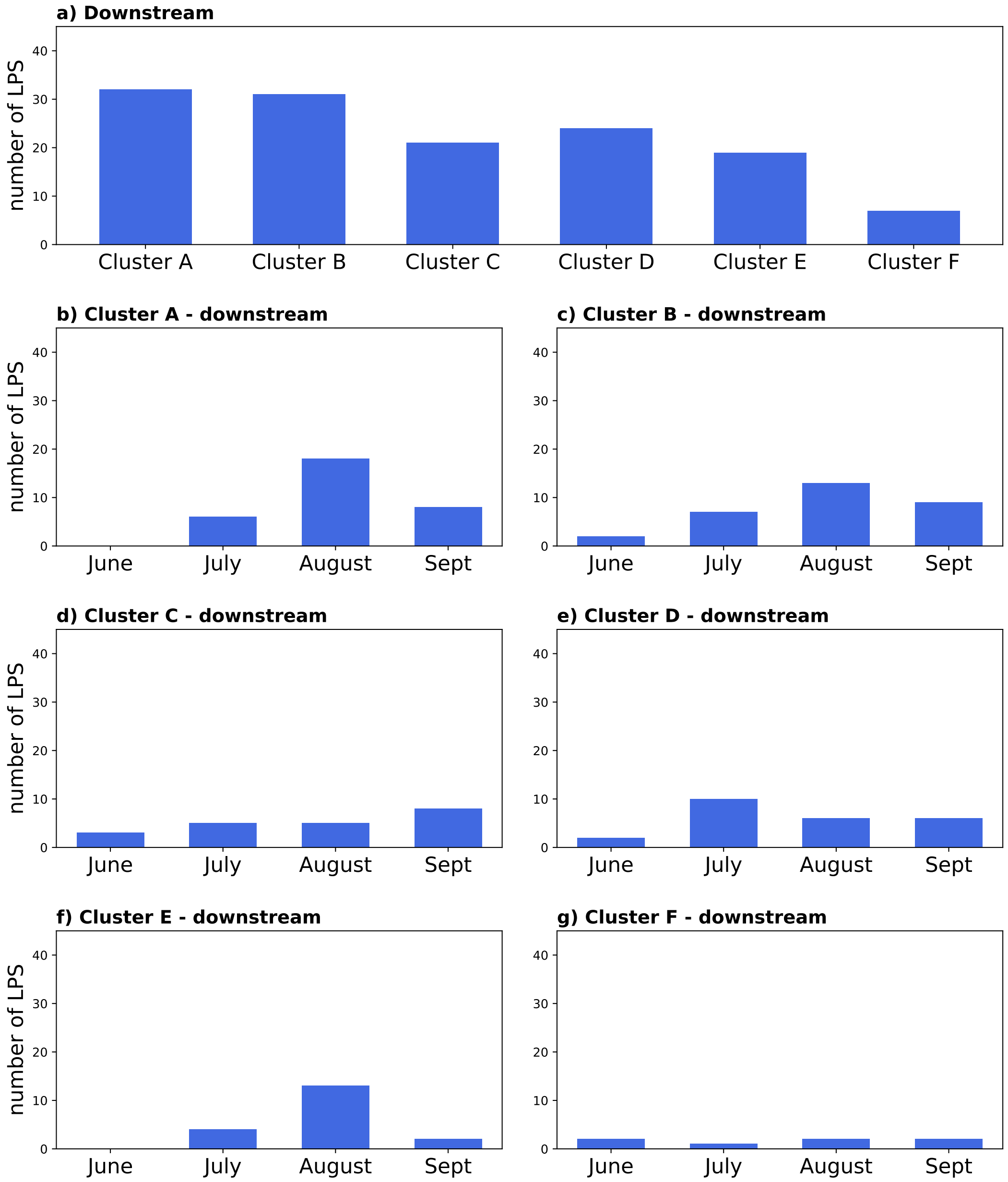

Figure 4. a) The number of downstream LPS associated with each TC cluster in the 10-day window prior to the initiation of the LPS.(b-g) monthly distribution of LPS for each TC cluster.

The composite ζ anomaly at 850 hPa from t-7 to t-0 days of downstream LPS cases are shown in Fig S4. A westward propagating positive ζ anomaly can be seen over central Pacific from seven days prior to the onset of a downstream LPS. This ζ anomaly intensifies over the WNP and propagates further west towards the BoB. The track densities of TCs in clusters A, B, C and D are high west of 140 °E which can be the reason for the intensification of ζ there.

4 Conclusion

The link between Western North Pacific (WNP) tropical cyclones (TCs) and the formation of downstream low-pressure systems (LPSs) over the Bay of Bengal is known since the late 1970s (Krishnamurti et al., 1977). However, a causal relationship between TC activity and downstream LPS genesis was not established. Here, we have established a causal relationship between WNP TCs and downstream LPS over the Bay of Bengal using transfer entropy. The prediction of monsoon LPS activity is highly desirable as these systems account for the synoptic scale variability that contributes more than half of the seasonal rainfall over the plains of continental India. Conventionally, the synoptic scale variability of Indian summer monsoon was considered chaotic, with low predictability (Goswami et al., 2006; S. K. Saha et al., 2019). The linkage between the WNP TC activity and downstream LPS genesis over the Bay of Bengal can lead to a new source of synoptic scale predictability of Indian summer monsoon. While it might not result in an immediate improvement in the predictability using conventional dynamical models, such a relationship can be useful for selecting predictors for data driven deep learning models. With the recent claims of synoptic-scale predictability by deep learning models (Sinha et al., 2021), a reliable prediction of downstream LPS genesis over the Bay of Bengal based on WNP TCs genesis might be possible.

Acknowledgments

K. S. S. Sai Srujan is supported by Prime Minister's Research Fellowship, Ministry of Education, Government of India.

Open Research

All data used in this study is freely available from public data repositories. Sea-level pressure data is available at `https://dx.doi.org/10.24381/cds.adbb2d47`. The tropical cyclone best track data can be obtained from `https://www.metoc.navy.mil/jtwc/jtwc.html?best-tracks`. The monsoon LPS data (Srujan et al., 2022) can be obtained from `https://doi.org/10.5281/zenodo.6331416`.

References

Blanford, H. (1890). The genesis of tropical cyclones. *Nature*, *43*, 81-83. doi: 10.1038/043081b0

Boos, W. R., Hurley, J. V., & Murthy, V. S. (2015). Adiabatic westward drift of Indian monsoon depressions. *Q J R Meteorol Soc*, *141*(689), 1035-1048. doi: https://doi.org/10.1002/qj.2454

Camargo, S. J., Robertson, A. W., Barnston, A. G., & Ghil, M. (2008). Clustering of eastern North Pacific tropical cyclone tracks: ENSO and MJO effects. *Geochemistry, Geophysics, Geosystems*, *9*(6). doi: https://doi.org/10.1029/2007GC001861

Camargo, S. J., Robertson, A. W., Gaffney, S. J., Smyth, P., & Ghil, M. (2007). Cluster analysis of typhoon tracks. part I: General properties. *Journal of Climate*, *20*(14), 3635–3653.

Chen, T.-C., & Weng, S.-P. (1999). Interannual and intraseasonal variations in monsoon depressions and their Westward-propagating predecessors. *Monthly Weather Review*, *127*(6), 1005 - 1020. doi: 10.1175/1520-0493(1999)127⟨1005:IAIVIM⟩2.0.CO;2

Cohen, N. Y., & Boos, W. R. (2016). Perspectives on moist baroclinic instability: Implications for the growth of monsoon depressions. *Journal of the Atmospheric Sciences*, *73*(4), 1767 - 1788. doi: 10.1175/JAS-D-15-0254.1

Deoras, A., Hunt, K., & Turner, A. (2021). The four varieties of south asian monsoon low-pressure systems and their modulation by tropical intraseasonal variability. *Weather*, *76*(6), 194–200.

Eliot, J. (1884). Account of southwest monsoon storms generated in the bay of bengal during 1877–1881. *Mem. Ind. Met. Dept*, *2*, 217–448.

Gaffney, S. J. (2004). *Probabilistic curve-aligned clustering and prediction with regression mixture models* (PhD dissertation). University of California, Irvine, CA.

Goswami, B. N., Wu, G., & Yasunari, T. (2006). The annual cycle, intraseasonal oscillations, and roadblock to seasonal predictability of the asian summer monsoon. *Journal of Climate*, *19*(20), 5078 - 5099. doi: 10.1175/JCLI3901.1

Gupta, M., Chauhan, T., Murtugudde, R., & Ghosh, S. (2020). Pollutants control the process networks of urban environmental-meteorology. *Environmental Research Letters*, *16*(1), 014021. doi: 10.1088/1748-9326/abce28

Hersbach, H., Bell, B., Berrisford, P., Hirahara, S., Horányi, A., Muñoz-Sabater, J., … others (2020). The era5 global reanalysis. *Q J R Meteorol Soc*, *146*(730), 1999–2049.

Hunt, K. M., & Fletcher, J. K. (2019). The relationship between indian monsoon rainfall and low-pressure systems. *Climate Dynamics*, *53*(3), 1859–1871.

Hurley, J. V., & Boos, W. R. (2015). A global climatology of monsoon low-pressure systems. *Q J R Meteorol Soc*, *141*(689), 1049-1064. doi: 10.1002/qj.2447

Kaiser, A., & Schreiber, T. (2002). Information transfer in continuous processes. *Physica D: Nonlinear Phenomena*, *166*(1), 43-62. doi: https://doi.org/10.1016/S0167-2789(02)00432-3

Kanamitsu, M., & Krishnamurti, T. N. (1978). Northern summer tropical circulations during drought and normal rainfall months. *Monthly Weather Review*, *106*(3), 331 - 347. doi: 10.1175/1520-0493(1978)106⟨0331:NSTCDD⟩2.0.CO;2

Krishnamurthy, V., & Ajayamohan, R. S. (2010). Composite structure of monsoon low pressure systems and its relation to Indian rainfall. *Journal of Climate*, *23*(16), 4285-4305. doi: 10.1175/2010JCLI2953.1

Krishnamurti, T. N., Molinari, J., lu Pan, H., & Wong, V. (1977). Downstream amplification and formation of monsoon disturbances. *Monthly Weather Review*, *105*(10), 1281 - 1297. doi: 10.1175/1520-0493(1977)105⟨1281:DAAFOM⟩2.0.CO;2

Liebmann, B., & Smith, C. A. (1996). Description of a complete (interpolated) outgoing longwave radiation dataset. *Bulletin of the American Meteorological Society*, *77*(6), 1275–1277.

Lindzen, R. S., Farrell, B., & Rosenthal, A. J. (1983). Absolute barotropic instability and monsoon depressions. *J. Atmos. Sci.*, *40*, 1178–1184.

Lizier, J. T., Prokopenko, M., & Zomaya, A. Y. (2008, Feb). Local information transfer as a spatiotemporal filter for complex systems. *Phys. Rev. E*, *77*, 026110. doi: 10.1103/PhysRevE.77.026110

Meera, M., Suhas, E., & Sandeep, S. (2019). Downstream and in situ: Two perspectives on the initiation of monsoon low-pressure systems over the Bay of Bengal. *Geophysical Research Letters*, *46*(21), 12303-12310. doi: https://doi.org/10.1029/2019GL084555

Mishra, S. K., & Salvekar, P. S. (1980). Role of baroclinic instability in the development of monsoon disturbances. *Journal of Atmospheric Sciences*, *37*(2), 383 - 394. doi: 10.1175/1520-0469(1980)037⟨0383:ROBIIT⟩2.0.CO;2

Murakami, T. (1980). Empirical Orthogonal Function analysis of satellite-observed outgoing longwave radiation during summer. *Monthly Weather Review*, *108*(2), 205 - 222. doi: 10.1175/1520-0493(1980)108⟨0205:EOFAOS⟩2.0.CO;2

Praveen, V., Sandeep, S., & Ajayamohan, R. S. (2015). On the relationship between mean monsoon precipitation and low pressure systems in climate model simulations. *Journal of Climate*, *28*(13), 5305-5324. doi: 10.1175/JCLI-D-14-00415.1

Saha, K., Sanders, F., & Shukla, J. (1981). Westward propagating predecessors of monsoon depressions. *Monthly Weather Review*, *109*(2), 330 - 343. doi: 10.1175/1520-0493(1981)109⟨0330:WPPOMD⟩2.0.CO;2

Saha, S. K., Hazra, A., Pokhrel, S., Chaudhari, H. S., Sujith, K., Rai, A., … Goswami, B. N. (2019). Unraveling the mystery of indian summer monsoon prediction: Improved estimate of predictability limit. *Journal of Geophysical Research: Atmospheres*, *124*(4), 1962-1974. doi: 10.1029/2018JD030082

Schreiber, T. (2000). Measuring information transfer. *Phys. Rev. Lett.*, *85*, 461–464. doi: 10.1103/PhysRevLett.85.461

Shukla, J. (1977). Barotropic & baroclinic instability of mean zonal wind during summer monsoon. *Pure Appl. Geophys.*, *115*, 1449–1461.

Shukla, J. (1978). Cisk-barotropic-baroclinic instability and the growth of monsoon depressions. *J. Atmos. Sci.*, *35*, 495–508.

Sinha, A., Gupta, M., Srujan, K. S. S. S., Kodamana, H., & Sandeep, S. (2021). Prediction of synoptic-scale sea level pressure over the Indian monsoon region using deep learning. *IEEE Geoscience and Remote Sensing Letters*, 1-5. doi: 10.1109/LGRS.2021.3100899

Sobel, A. H., & Bretherton, C. S. (1999). Development of synoptic-scale disturbances over the summertime tropical northwest Pacific. *Journal of the Atmospheric Sciences*, *56*(17), 3106–3127.

Srujan, K. S. S. S., Sandeep, S., & Suhas, E. (2021). Downstream and in situ genesis of monsoon low-pressure systems in climate models. *Earth and Space Science*, *8*(9), e2021EA001741.

Srujan, K. S. S. S., Sandeep, S., Suhas, E., & Kodamana, H. (2022, March). *Tracks of Indian Summer monsoon Low-Pressure Systems from ERA5.* Zenodo. Retrieved from `https://doi.org/10.5281/zenodo.6331416` doi: 10.5281/zenodo.6331416

Tam, C.-Y., & Li, T. (2006). The origin and dispersion characteristics of the observed tropical summertime synoptic-scale waves over the western Pacific. *Monthly Weather Review*, *134*(6), 1630–1646.

Thomas, T. M., Bala, G., & Srinivas, V. V. (2021). Characteristics of the monsoon low pressure systems in the indian subcontinent and the associated extreme precipitation events. *Climate Dynamics*, *56*(5), 1859–1878.

Webster, P. J., & Chang, H.-R. (1988). Equatorial energy accumulation and emanation regions: Impacts of a zonally varying basic state. *Journal of the Atmospheric Sciences*, *45*(5), 803–829.

Wheeler, M., & Kiladis, G. N. (1999). Convectively Coupled Equatorial Waves: Analysis of Clouds and Temperature in the Wavenumber–Frequency Domain. *Journal of the Atmospheric Sciences*, *56*(3), 374-399. doi: 10.1175/1520-0469(1999)056⟨0374:CCEWAO⟩2.0.CO;2

Supporting Information for "A dynamical linkage between Western North Pacific tropical cyclones and Indian monsoon low-pressure systems"

K. S. S. Sai Srujan[1], S. Sandeep[1], E. Suhas[2], and Hariprasad Kodamana[3,4]

[1]Centre for Atmospheric Sciences, Indian Institute of Technology Delhi, New Delhi 110016, India

[2]Earth and Climate Science, Indian Institute of Science Education and Research Pune, Pune 411 008, India

[3]Department of Chemical Engineering, Indian Institute of Technology Delhi, New Delhi 110016, India

[4]School of Artificial Intelligence, Indian Institute of Technology Delhi, New Delhi 110016, India

Contents of this file

Table S1. Mean angle of re-curvature of TCs in each cluster

Clusters	***Angle (degrees)***
A	63.08
B	0
C	87.05
D	0
E	81.05
F	101.38

Table S2. The statistics of Western North Pacific TCs that had genesis during June to September in 1979 - 2017 period.The clusters are in decreasing order with respect to number of TCs in the cluster.

Cluster	***No. of TCs***	***% of TCs***	***No. landfalling TCs***	***% of landfalling TCs***
A	149	23.9	18	12.1
B	144	23.1	127	88.2
C	102	16.3	28	27.5
D	86	13.8	83	96.5
E	80	12.8	3	3.8
F	63	10.1	13	20.6
All	624	100%	272	43.6%

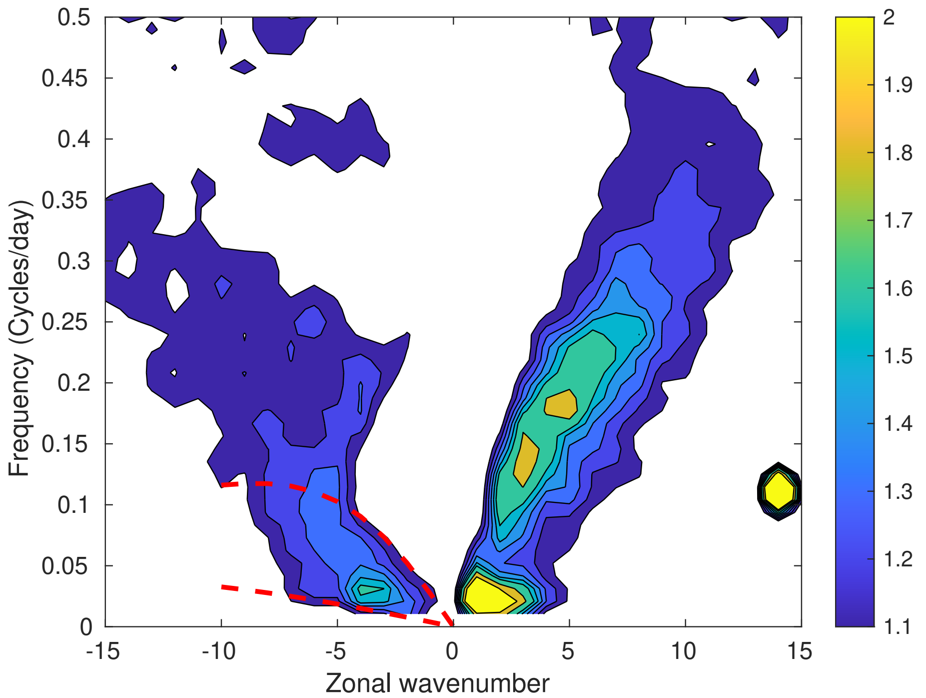

Figure S1. The Wheeler Kiladis symmetric/background wavenumber-frequency spectra of daily outgoing longwave radiation anomaly from 1979 to 2017 (June-September). Red lines represent theoretical dispersion for n=1 Rossby waves for an equivalent depth equal to 10 m and 100 m, respectively.

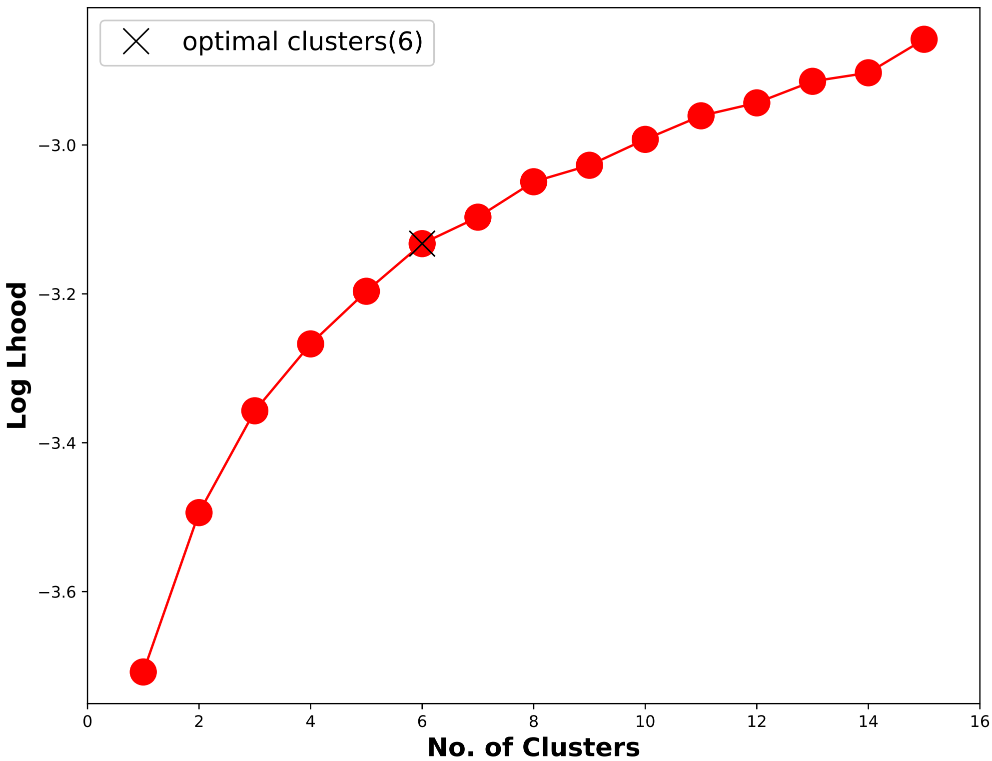

Figure S2. The log-likelihood values for the different number of clusters (1-15 clusters). The log-likelihood values shown are the maximum of 20 runs, obtained by a random permutation of the 70% tropical cyclones given to the cluster model. This analysis is done for June – September period during 1979 – 2017.

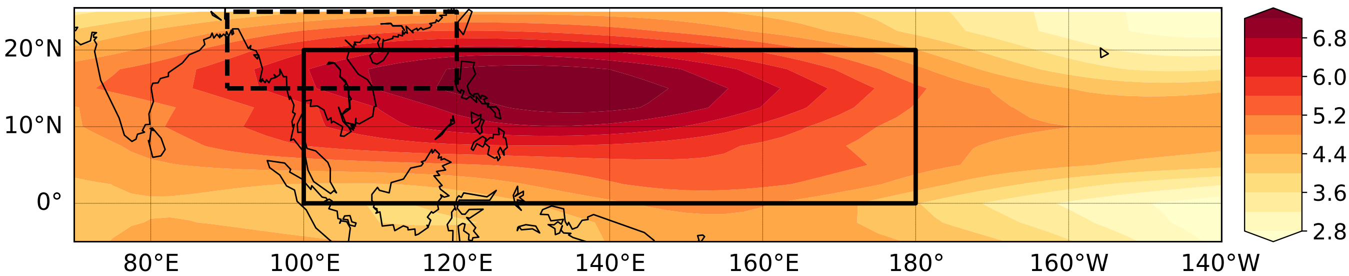

Figure S3. Mean Rossby variance of outgoing longwave radiation for JJAS during 1979 - 2017. The solid (dashed) box is the box2 (box1) respectively for which TE is computed.

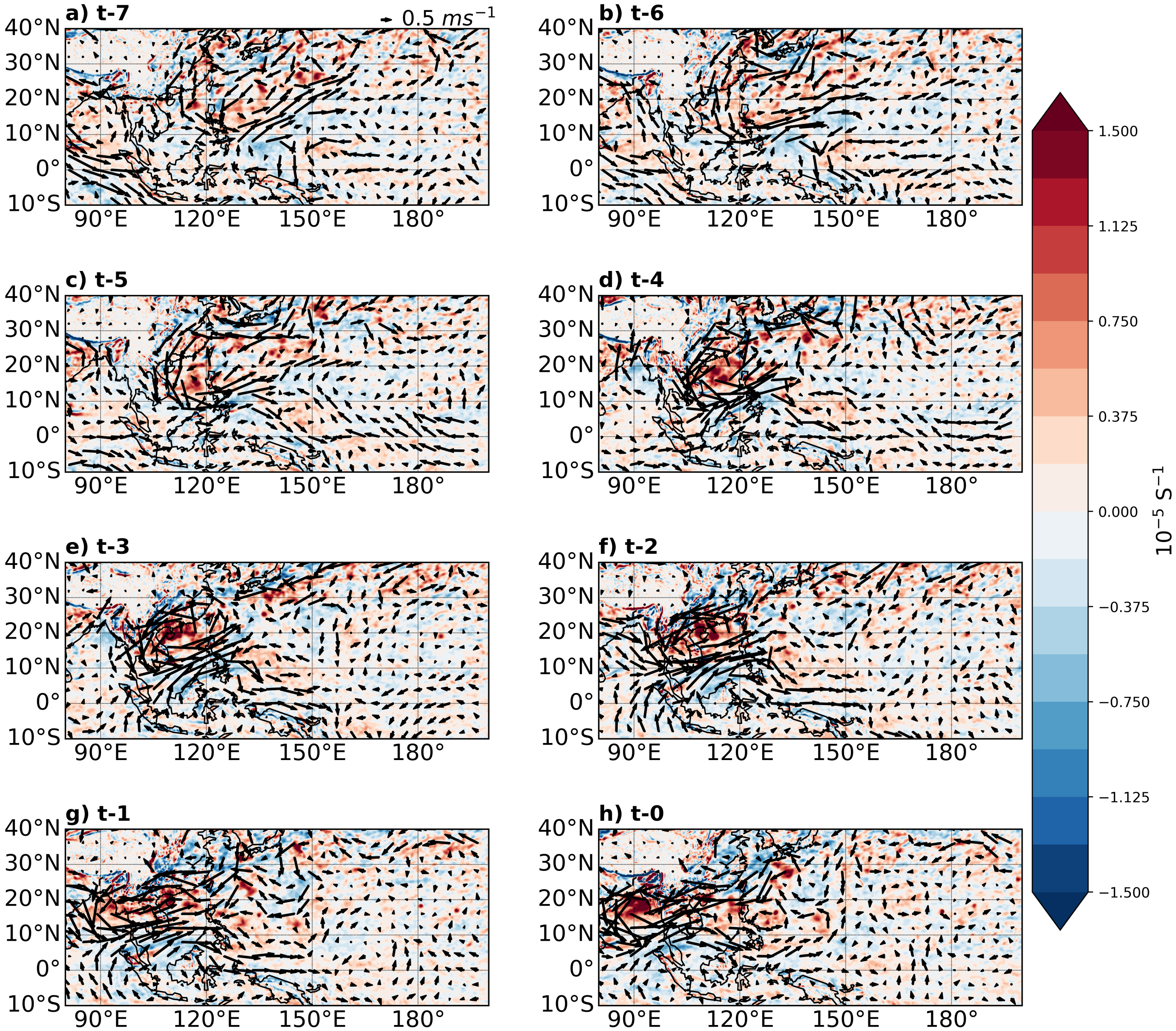

Figure S4. Composites of wind vectors and relative vorticity anomaly at 850 hPa over the Pacific from t-7 to t-0 (a-h) for the downstream LPS, where t-0 corresponds to the day of downstream LPS genesis. This analysis is done for June – September period during 1979 – 2017.

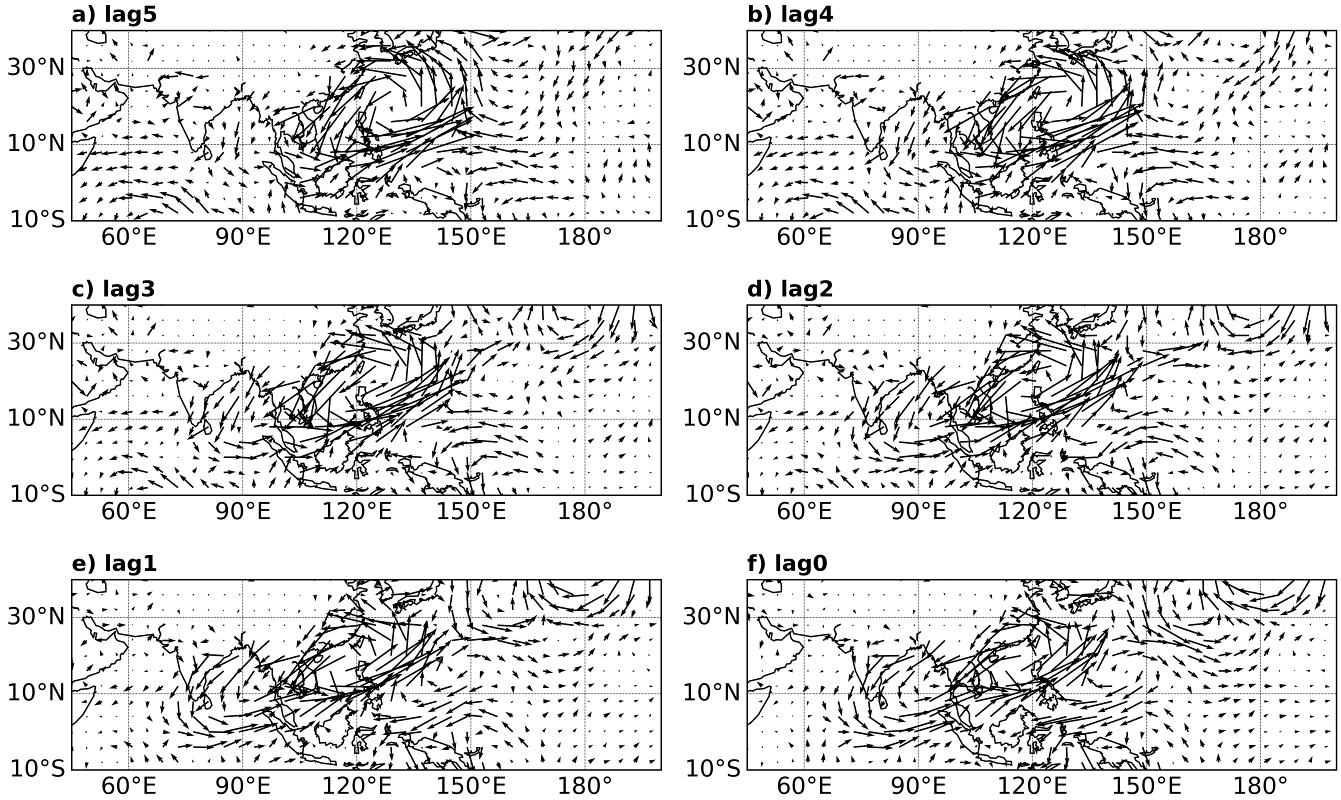

Figure S5. Regression of 850 hPa wind vectors on PC1 of the Rossby filtered outgoing longwave radiation from lag-5 to lag-0 (a-f). At lag0 both the time series are considered from t-0 to t-10 for each downstream LPS where t-0 is the day of genesis of downstream LPS. At each lag, the PC1 time series is lagged behind the wind vector time series. The units of regression coefficients are m s^{-1}(std of PC1)$^{-1}$. This analysis is done for June – September period during 1979 – 2017.

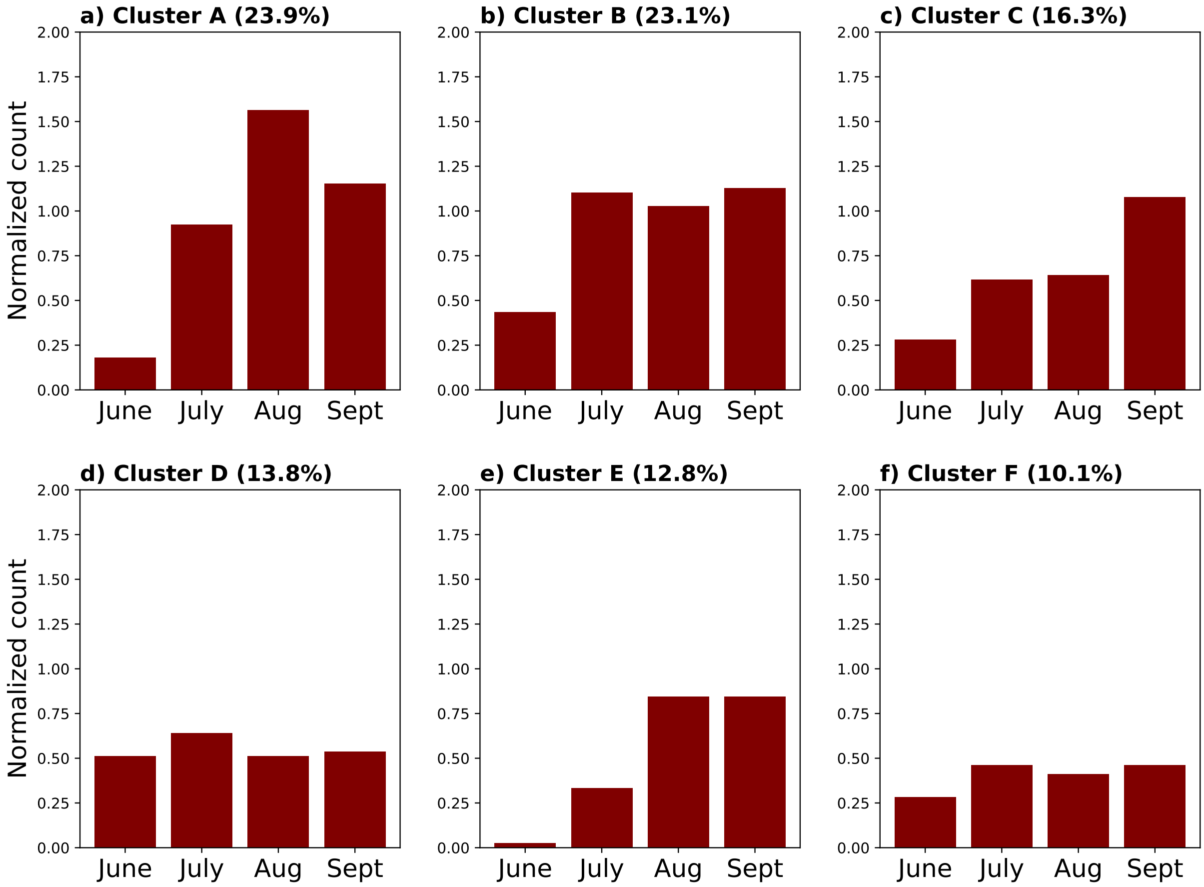

Figure S6. The Normalized monthly distribution of TCs in each cluster from A-F. This analysis is done for 1979 – 2017. The percentage of TCs in each cluster are mentioned on top of figure from a-f

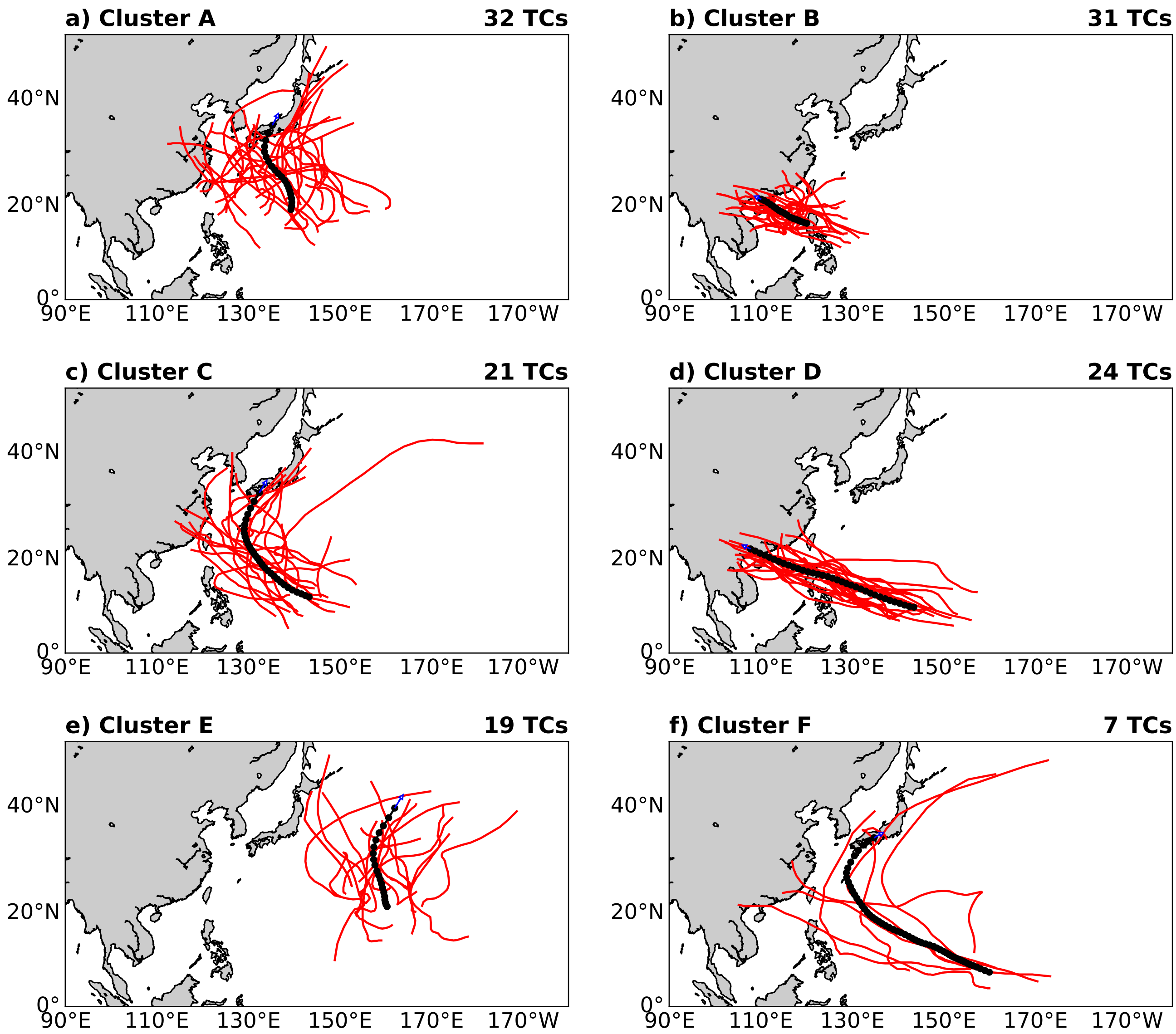

Figure S7. The tracks of TCs over WNP from 1979-2017 which triggers downstream LPS in each cluster from A-F with the mean track(Black line) of TCs interpolated to a length of 5 days. The number of TC tracks in each cluster is indicated on top right side of the panels. This analysis is done for June – September period during 1979 – 2017.

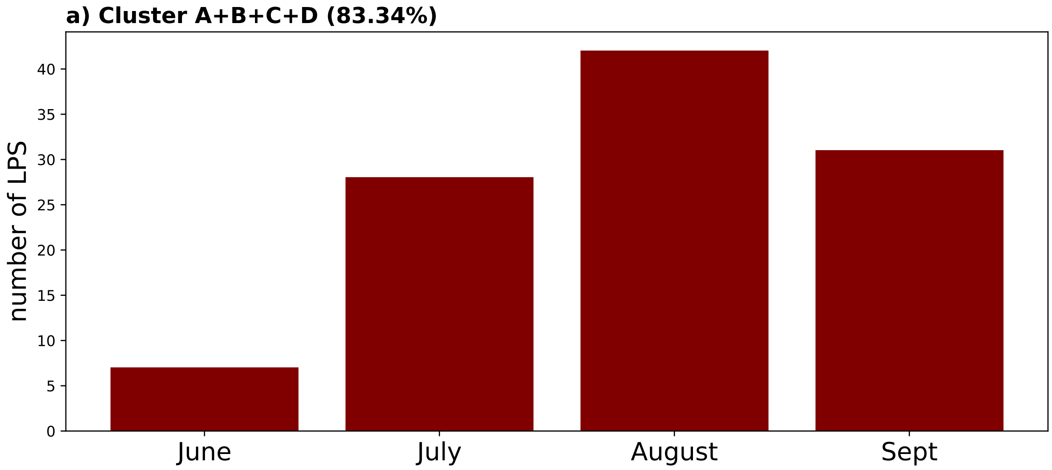

Figure S8. Sum of monthly distribution of LPSs in clusters A,B,C, and D. The number of unique LPS in these four clusters are account to 83.34%. This analysis is done for June – September period during 1979 – 2017.